 CMES, vol.89, no.2, pp.97-109, 2012

An Analysis of The Flow Resistance in Coiled Tubing Wound Around A Reel, In Microhole Drilling

Xuejun Hou[1,2], **Deli Gao**[1] **and Zhonghou Shen**[1]

Abstract: Microhole drilling (MHD) is a new frontier drilling technology in which the diameter of wellbore is less than 88.9mm and coiled tubing (CT) is used as drill string. The CT wound around reel for MHD has small bending radius and large length to result in large circulating flow resistance and affect normal MHD circulation. The calculation model for curvature radius and length of CT wound around reel are established by analyzing the relationships among the various geometrical parameters of the reel system. The calculation model is combined with Dean number and power-law fluid state equation to put forward the calculation model for the flow resistance in CT wound around reel (CTFR), which takes into changes of the parameters such as flow rate & density of drilling fluid, inner diameter & length of CT and the reel diameter. The calculation result shows that CTFR is considerably affected by the diameter & length of CT and drilling fluid flow rate. CTFR increases rapidly with reducing of the CT diameter and increasing of the CT length and drilling fluid flow rate. Simultaneously, it is significantly affected by the circulation drilling fluid density in CT. With increasing of circulating drilling fluid density, CTFR increases significantly. The higher the flow rate is, the larger the CTFR increment is. The research results may be useful for MHD parameter selections related to CTFR.

Keywords: microhole drilling; coiled tubing; reel system; flow resistance; power-law fluid

1 Introduction

MHD is a kind of a new frontier in drilling technology, in which the wellbore diameter is less than 88.9 mm, and a CT is used as the drill string. Compared

[1] State Key Laboratory of Petroleum Resource and Prospecting, China University of Petroleum, Beijing 102249, China. Corresponding author: Deli GAO, E-mail: gaodeli@cup.edu.cn

[2] College of Petrol Engineering, Chongqing University of Science and Technology, Chongqing 401331, China.

with conventional drilling, MHD is safer, more effective, lower in operating costs and easily amenable automation [Li Hui (2008)]. In 1994, the concept of drilling deep small holes with diameters from 2-3/8-in to 1-3/8-in was presented by the United States Los Alamos National Laboratory [Albright (2005)]. Dreesen and Cohen (1997) had conducted a feasibility investigation of the deep MHD by using laboratory-scale microdrilling demonstrations. In 1999, the USA Department of Energy (DOE) started to support the R&D work of MHD technology. The DOE (2004) invested $5.6 million for six MHD research projects. The DOE (2005) invested $14.5 million for second batch of MHD research projects. Thus, there has been a considerable progress in MHD technology [Perry (2006)].

However, MHD has a small size borehole, and a high resistance in the circulating flow of the drilling fluid. The whole MHD flow resistance mainly consists of a surface CTFR, flow resistance in downhole CT, hydraulic resistance at bit, and flow resistance in the hole annular, of which the last three factors have been taken into account in hydraulic designs made for CT drilling [Walton (1996)]. A new approach was presented for predicting the flow resistance of a non-Newtonian fluid in CT [Medjani (2000)]. A computational method was studied for Newtonian fluid flow resistance in spiral CT [Srinivasan (1970)]. Correlations of frictional pressure were presented for turbulent flows of polymer solutions, in straight and spiral CT [Gallego (2009)]. Frictional pressures were studied for Newtonian and non-Newtonian fluids in straight and reeled CT [Willingham (2000)]. Fluid-flow in CT from reel to injector was simulated by CFD software [Bailey (2009)]. Circulating flow resistance in CT of ultra-short radius drilling was studied [Ma (2012)]. However, there is very little literature reporting the research on CTFR in MHD. In this paper, geometric parameters of the reel system will be identified, to build the computational models for the radius of curvature and length of CT wound around reel; the computational models for CTFR will be established in light of the Dean number and flow state equation of power law fluid; the characteristics of the changes in CTFR will be analyzed by computations corresponding to different flow rates & density of the drilling fluid, inner diameter & length of CT, and the reel diameter. The research results are useful for selecting the MHD parameters related to CTFR.

2 A Simplified Model for the Reel System CT

The CTFR analysis is mainly focused on the CT wound around a reel in MHD. However, the CTFR varies with different parameters such as the reel diameter, the layer number, inner diameter, bending radius and length of CT, and the flow rate, density and the coefficient of viscosity of the drilling fluid, etc. A simplified model of the CT wound around a reel is built for a simplified CTFR analysis, as shown in the Fig.1 below.

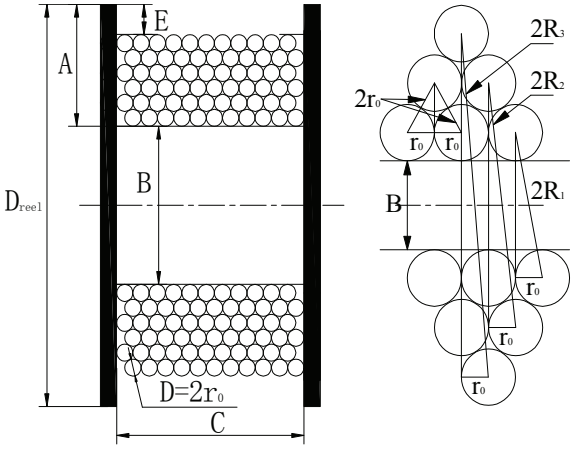

Figure 1: The simplified analysis model of CT wound around a reel

According to the simplified model of CT wound around a reel, as shown in Fig.1, the formulas for computing the CT parameters are derived as follows

$$\begin{cases} N = \left[\frac{A-E}{D}\right] \\ M = \left[\frac{C}{D}\right] = \left[\frac{C}{2r_0}\right] \\ D_{reel} = B + 2A \\ R_i = \frac{\sqrt{\left[(2r_0+B)+2\sqrt{3}(i-1)r_0\right]^2+r_0^2}}{2} \quad (N \geq i \geq 1) \\ L = 2\pi M \sum_{i=1}^{N} R_i \\ L_i = 2\pi M R_i \end{cases} \tag{1}$$

where, N, an integer, is the number of layers of CT wound around a reel; A is the height of of the flange of the reel system, m; E is distance from the outermost CT wound around the reel to outer rim of reel system, m; M, an integer, is the number of columns of each layer of CT wound around the reel; D is the outer diameter of CT, m; C is the width of the rim of the CT reel, m; r_0 is radius of CT, m; D_{reel} is the outer diameter of the reel system, m; B is the outer diameter of reel, m; R_i is the radius of curvature for the ith layer of CT wound around the reel, m; L_i is length of the ith layer of CT wound around the reel, m; L is total length of all CT wound around the reel, m.

The diameter of the reel is so small that a long CT wound around the reel has a very small radius of curvature in bending. When a non-Newton fluid flows in a long CT wound around a reel, a secondary Dean vortex appears under the interaction

of the viscous force and the centrifugal force, which will produce a big CTFR so that the resulting CTFR is much more than flow resistance in straight CT. Dean (1927 and 1928) studied the motion of a fluid in a curved pipe and put forward the dimensionless Dean number to measure the intensity of the Dean vortices. The Dean number is the influence coefficient of drilling fluid CTFR. The formula for computing the Dean number is as follows:

$$N_{Dn} = Re\left[\frac{r_0}{R_i}\right]^{0.5} \tag{2}$$

where, Re is the dimensionless Reynolds number; N_{Dn} is the dimensionless Dean number, which is the ratio of centrifugal force to viscous force; other symbols are the same as the above.

3 A Model for the Computation of CTFR

3.1 Power Law Rheological Equation

In conventional drilling, the actual rheological properties of the drilling fluid curves are usually approximated by the power law rheological model. This model is used to calculate CTFR, in which the rheological equation, parameters and the computational models [Liu (1998)] are listed as follows:

$$\begin{cases} \tau = K_p\left(\frac{du}{dy}\right)^{n_p} \\ n_p = 3.322\log_{10}\left(\frac{\phi_{600}}{\phi_{300}}\right) \\ K_p = \frac{0.511\phi_{600}}{1022^{n_p}} \end{cases} \tag{3}$$

where, ϕ_{600} is the reading of the rotary viscosimeter while its rotary speed is 600r/min; ϕ_{300} is the indication of the rotary viscosimeter while its rotary speed is 300r/min; K_p is consistency coefficient of the power-law fluid and it is dependent on the properties of the drilling fluid, $\mathrm{P}_a \times \mathrm{s}^n$; n_p is the behavior index (liquidity index) of power-law a fluid, dimensionless, and it represents the degree to which it deviates from the Newtonian fluid; τ is the shear stress, Pa; and the other symbols are the same as the above.

3.2 Calculation of the Reynolds Number

Reynolds number is the ratio of inertia force to viscosity force, and it is also the basis used to judge the flow regime of the drilling fluid. For the power-law fluid

flowing in CT, its equation can be described follows:

$$Re = \frac{\rho d^{n_p} v_p^{2-n_p}}{8^{n_p-1} K_p \left(\frac{3n_p+1}{4n_p}\right)^{n_p}} \tag{4}$$

where, d is the CT inner diameter, m; v_p is the average flow velocity of the drilling fluid, m/s; ρ is the density of drilling fluid, kg/m^3; and the other symbols are the same as the above.

3.3 Definitions of Flow-Regimes, and the Computation of the Flow Resistance Coefficient

Assuming that the discriminating factors C_1 and C_2 are computed by the equation (5), the flow regime and its friction resistance coefficient [Gallego (2009)] can be determined by comparing the values of Reynolds number with C_1 and C_2.

$$\begin{cases} C_1 = 3470 - 1370 n_p \\ C_2 = 4270 - 1370 n_p \end{cases} \tag{5}$$

(1) When $Re < C_1$, the state of flow of the drilling fluid in CT wound around a reel is laminar, and its corresponding Fanning friction factor can be calculated by the following equation:

$$\begin{cases} f = \frac{16}{Re} \\ f_i = \frac{16}{N_{Dn}} \end{cases} \tag{6}$$

where, f is the Fanning friction factor for laminar flow in the straight CT, dimensionless; f_i is the Fanning friction factor [Rao (2000)] of laminar flow in the ith layer of CT, dimensionless; other symbols are the same as the above.

(2) When $Re > C_2$, the state of flow of the drilling fluid in CT wound around a reel is turbulent, and its corresponding Fanning friction factor [Rao (2000)] can be calculated by the following equations:

$$\begin{cases} f = \frac{a}{Re^b} \quad \& \quad f_i = \frac{a}{N_{Dn}^b} \\ a = \frac{\lg n_p + 3.93}{50} \\ b = \frac{1.75 - \lg n_p}{7} \end{cases} \tag{7}$$

where, f is the Fanning friction factor of turbulent flow in straight CT, dimensionless; f_i is the Fanning friction factor of turbulent flow in ith layer of CT, dimensionless; a and b are the calculation coefficients; other symbols are the same as the above.

(3) When $C_1 \leq R_e \leq C_2$, state of the drilling fluid in CT wound around a reel is that of transition flow, and its corresponding Fanning friction factor [Rao (2000)] can be calculated by the following equations:

$$\begin{cases} f = \frac{16}{C_1} + \left(\frac{a}{C_2^b} + \frac{16}{C_1}\right) \frac{Re - C_1}{800} \\ f_i = \frac{16}{C_1} + \left(\frac{a}{C_2^b} + \frac{16}{C_1}\right) \frac{N_{Dn} - C_1}{800} \end{cases} \tag{8}$$

where, f is the Fanning friction factor of transition flow in the straight CT, dimensionless; f_i is the Fanning friction factor of transition flow in ith layer of CT, dimensionless; other symbols are the same as the above.

3.4 A Model for the Computation of CTFR

According to the parametric analysis of the simplified reel model and Fanning equations, the models for the computation of CTFR can be described as follows:

$$\begin{cases} \Delta p_s = \frac{2\rho v_p^2}{d} fL \\ \Delta p_r = \frac{2\rho v_p^2}{d} \sum\limits_{i=1}^{N} (f_i L_i) \end{cases} \tag{9}$$

where, Δp_s is the flow resistance in a straight CT with L length, while the flow of power-law fluid is laminar, Pa; Δp_r is the total flow resistance in all CT wound around a reel, while the flow of power-law fluid is laminar, Pa; other symbols are the same as the above.

4 Numerical Analysis of CTFR

4.1 Parameters for Computations

The CT wound around a reel is easy to undergo flexural deformations. The deformation is determined by the sizes of the CT and the reel. The reel diameter is generally more than 48 times the diameter of the CT. According to the available CT (shown in Table 1) used in microhole with 89mm diameter, the following parameters of the CT and the reel are listed in Table 2. It is assumed that drilling fluid density with low solid content, and low viscosity, is 1.5g/cm^3, the rotary viscosimeter indication ϕ_{600} is 35 when its rotary speed is 600r/min, the rotary viscosimeter indication ϕ_{300} is 12 when its rotary speed is 300r/min and the rotary viscosimeter indication ϕ_3 is 3 when its rotary speed is 3r/min. Thus, the CTFR is calculated for a microhole with 89mm diameter by the above equations (1) $\sim$ (9).

Table 1: CT parameter tables [Zhao (2011)]

Outer Diameter (mm)	25.4	31.750	38.100	44.450	50.800	60.325	73.025	88.900
Inner Diameter (mm)	19.05	23.826	30.176	36.526	42.876	52.401	65.101	80.976

Table 2: Parameter tables of the reel system [Li (2003)]

Size Parameters of Reel System (m)			D (mm)	25.4	31.75	38.1	44.45	50.8	60.325	73.025
			E (mm)	50.8	50.8	50.8	69.85	76.2	88.9	101.6
Reel System Outer Diameter	Flange Height	Reel Diameter	Reel System Width (m)	L (m) Total Length of CT Wound Around Reel						
D_{reel}	A	B	C							
3.91	0.787	2.337	1.651	17430	11526	7857	5670	3918	2800	1863
3.91	0.711	2.489	1.651	15950	10208	7204	5064	3738	2623	1699
4.06	0.61	2.845	2.007	18587	11390	7727	5732	4109	2760	1671
4.57	0.864	2.845	2.261	32730	20293	14190	9616	7480	4979	3370
4.57	0.635	3.302	2.261	24994	15553	10771	7230	5871	4023	2516

4.2 Analysis of the Computed Results

(1) CTFR Related to Flow Rate and CT Diameter

It is assumed that CT with 2000m length and different diameters is wound around the reel with 2.845m diameter, and the flow rate of the drilling fluid varies from 1m/s to 5m/s. Thus, the computed results for the CTFR are illustrated in Fig.2.

The CTFR increases nonlinearly with the increasing of the flow rate, and its increase is obvious. The larger the inner diameter of the CT is, the smaller the CTFR is, but the CTFR-reduction curve is tending to be flat with an increase in the CT inner diameter.

When the flow rate is less than 4m/s, the CTFR is the smallest for 88.9mm diameter CT, and its value is 12.94MPa, but the CT can't be used for the 88.9mm diameter microhole because of the zero annulus size. The highest CTFR occurs in 73.025mm diameter CT, and its value is 17.64MPa. When the flow rate is 3m/s, the maximum theoretical CTFR is about 10.22MPa for 73.025mm diameter CT, and 13.91MPa for 60.325mm diameter CT. Thus, if the flow rate is lower, the CTs with smaller diameters such as 73.025mm and 60.325mm can be used in MHD.

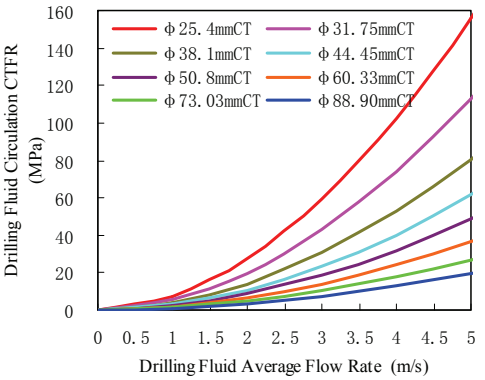

Figure 2: Curves of CTFR changing with flow rate in 2000m length CT wound around the reel with 2.845 m diameter

(2) CTFR Related to Flow Rate and CT Length

It is assumed that the CT is wound around the reel with 2.845m diameter, the diameter of CT is 73.025mm, its length varies from 0m to 4000m. Thus, the computed results for CTFR are illustrated in Fig.4.

The CTFR increases linearly with the increasing of the CT length. The longer the CT is, the larger the CTFR increment is. The CTFR increases with the increasing of flow rate. Considering the capacity of the surface pumping equipments, the flow

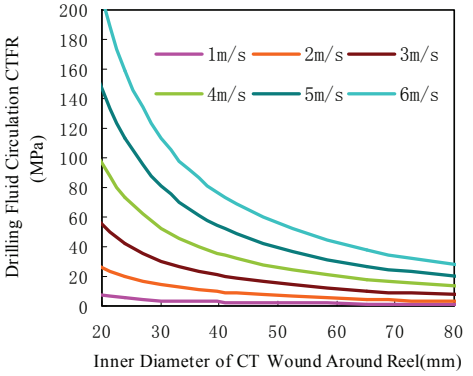

Figure 3: Curves of CTFR changing with inner diameter of 2000m length CT wound around the reel with 2.845m diameter

rate of drilling fluid in the 73.025mm diameter CT is 8m/s when its length is 500m, and decreases to 5m/s when its length is 1000m; the maximum flow rate is 4m/s when its length is between 1500m and 2000m, and the flow rate is only 3m/s while its length is between 2500m and 3000m, and it is 2m/s while between 3500m and 4000m.

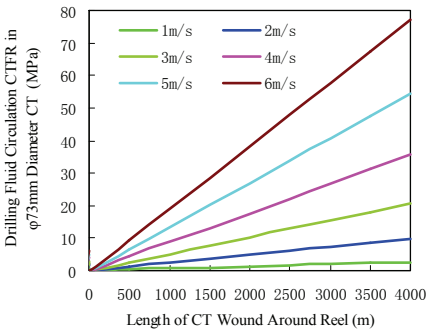

Figure 4: Curves of CTFR with length of CT wound around reel

(3) Relation of CTFR to the Reel Diameter

A CT with 73.025mm diameter & 2000m length is assumed to be wound around the reel with diameters of 2.337m, 2.489m, 2.845m and 3.302m, and the computed results of CTFR are shown in Fig.5 and Fig.6.

With the increasing of the reel diameter from 1.2m to 3.3m, the CTFR increases, but the increment is very little. With the increasing of drilling fluid flow rate, the

CTFR increases. The change of the radius of curvature is smaller, because of the change of the reel diameter from 1.2m to 3.3m. Thus, the selections of CT and the reel system are mainly dependent on the minimum radius of bending curvature of the CT and loads, volume & height of the reel system, as shown in Fig.5.

The CTFR is mainly affected by the flow rate. The higher the flow rate is, the higher the CTFR is, and the higher increment is too (Fig.5).

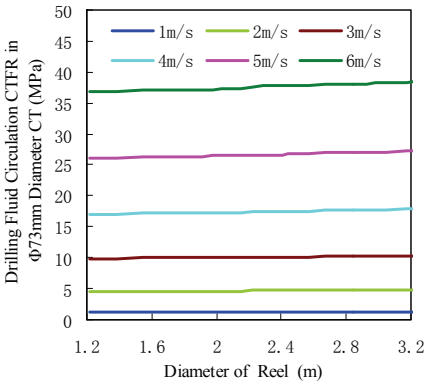

Figure 5: Curves of CTFR changing with the reel diameter for 2000m length CT with 73.025m diameter

Compared with the flow resistance in straight CT, the CTFR is seriously affected by bending effects of CT wound around reel. The CTFR is much larger than the flow resistance in the straight CT. With the increasing of the inner diameter of the CT, the ratio of CTFR to the flow resistance in straight CT reduces. When the CT inner diameter increases from 20mm to 80mm, the ratio reduces from 1.69 to 1.50, as shown in Fig.6.

(4) CTFR Related to Drilling Fluid Flow

CT with 73.025mm diameter & 2000m length is considered to be wound around the reel, with 2.845m diameter. When the flow velocity and density of drilling fluid vary, the computed results for CTFR are shown in Fig.7. The CTFR in CT with 73.025mm diameter increases linearly with the increasing of drilling fluid density, while the other conditions are constants. The increment of CTFR is obvious when the flow rate is higher. Thus, The CTFR can be reduced with the decreasing of the drilling fluid density in 89mm diameter MHD.

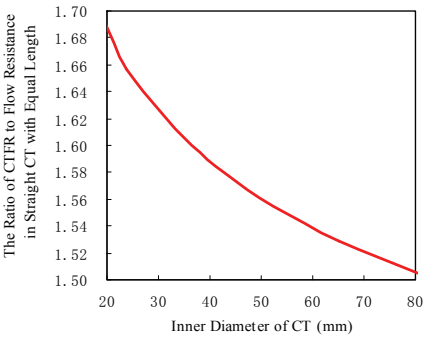

Figure 6: Curve about ratios of CTFR to flow resistance in straight line CT

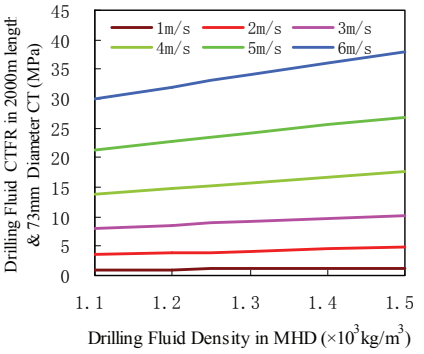

Figure 7: Curves of the CTFR changing with density and flow rate of drilling fluid

5 Conclusions

(1) The CTFR is considerably affected by the inner diameter & length of CT, and by the flow rate of the drilling fluid in MHD. With the decreasing of CT inner diameter, and the increasing of CT length and the flow rate, the CTFR increases rapidly. In the allowable pressure range of drilling pump equipment, it is possible to reduce the CTFR by increasing CT inner diameter and reducing the flow rate in MHD.

(2) When the reel diameter reduces from 1.2m to 3.3m, the CTFR increment is very little. With the increasing of drilling fluid flow rate, rate of increase of CTFR is higher. Compared with the flow resistance in a straight line CT, the CTFR is seriously affected by the bending effects of CT wound around a reel. With the increasing of the CT inner diameter, the ratio of CTFR to the flow resistance in straight CT is reduced.

(3) The CTFR is significantly affected by the density of the drilling fluid in MHD. With the increasing of the density of the drilling fluid, the CTFR increases significantly. The higher the flow rate is, the larger the CTFR increment is. Therefore, the CTFR can be reduced by reducing appropriately the drilling fluid density in MHD.

Acknowledgement: The authors gratefully acknowledge the financial support of the Natural Science Foundation of China (NSFC: 51221003). This research was also supported by the other projects (Grant numbers: 2010CB226703, 2011ZX05009, 2011A-4208).

References

Albright, J.; Dreesen, D.; Anderson, D.; Blacic, J.; Thomson, J.; Fairbanks, T. (2005): Road Map for a 5000-ft microborehole. *Los Alamos National Laboratory*. pp.1-5.

Bailey, M.; Blanco, I. L.; Rosine, R. S. (2009): Comparison of Computional fluid Dynamics of Erosion in Coiled Tubing on Reel-to-Injector Flow Area. *SPE* 121171.

Dean, W. R. (1927): Note on the Motion of Fluid in a Curved Pipe. *Philosophical Magazine*, vol. (20), pp.208-223.

Dean, W. R. (1928): Fluid Motion in a Curved Channel. Proceedings of the Royal Society of London: Series A, vol. 121(787), pp.402-420.

DOE, (2004): DOE to Support "Small Footprint" Technologies for Oil and Gas Fields. www.fossil.energy.gov.

DOE, (2005): DOE Announces R&D funding for microhole technology projects.

www.fossil.energy.gov.

Dreesen, D. S.; Cohen, J. H. (1997): Investigation of The Feasibility of Deep Microborehole Drilling. *Proceedings of 8th Annual Energy Week Conference and Exhibition*, vol. I, Book III Houston, TX, pp. 137-144.

Gallego, F.; Shah, S. N. (2009): Friction pressure correlations for turbulent flow of drag reducing polymer solutions in straight and coiled tubing. *Journal of Petroleum Science and Engineering*, vol. 65(3/4), pp. 147-161.

Li, H.; Huang, B. S.; Liu, Q. Y. (2008): Micro-borehole Drilling Technology and Its Application Prospect. *Drilling & Production Technology*, vol.31(2), pp. 42-45.

Liu, H. L.; Ke, Z. H.; Zhao, Z. F. (1998): Development and Application on Slimhole and Coiled Tubing Technology. *Beijing: Petroleum Industry Press*, pp. 40-41.

Li, Z. T. (2003): Coiled Tubing Technical Manual. *Beijing: Petroleum Industry Press*, pp.156-157.

Ma, D. J.; Li, G. S.; Huang, Z. W.; Niu, J. L.; Hou, C.; Liu, M. J.; Li, J. B. (2012): A model of calculating the circulating pressure loss in coiled tubing ultra-short radius radial drilling. *Petroleum Exploration and Development*, vol. 39(4), pp.528-533.

Medjani, B.; Shah, S. N. (2000): A New Approach for Predicting Frictional Pressure Losses of Non-Newtonian Fluid in Coiled Tubing. *SPE* 60319.

Perry, K.; Bataresh, S.; Gowelly, S.; Hayes, T. (2006): Field demonstration of exiting microhole coiled tubing rig (MCTR) technology final technical report. *Gas Technology Institute*, pp. 1-8

Rao, B. N. (2000): Friction Factors for Turbulent Flow of Non-Newtonian Fluids in Coiled Tubing. *SPE* 74847

Srinivasan, P. S.; Nandapurkar, S. S.; Holland, F. A. (1970): Friction factors for coils. *Transactions of the Institution of Chemical Engineers*, vol.48(1), pp.156-161.

Walton, I. C.; Gu, H. (1996): Hydraulics Design in Coiled Tubing Drilling. *SPE* 36349.

Willingham, J. D.; Shah, S. N. (2000): Friction Pressures of Newtonian and Non-Newtonian Fluid in Straight and Reeled Coiled Tubing. *SPE* 60719.

Zhao, Z. M. (2011): Coiled Tubing Engineering Technical Manual. *Beijing: Petroleum Industry Press*, pp. 71-78.